Oecologia (2022) 198:889–904
https://doi.org/10.1007/s00442-022-05150-7

METHODS

Nonlinear spatial and temporal decomposition provides insight for climate change effects on sub-Arctic herbivore populations

Hannah E. Correia[1,2] · Torkild Tveraa[3] · Audun Stien[4] · Nigel Yoccoz[3,4]

Received: 23 October 2021 / Accepted: 6 March 2022 / Published online: 24 March 2022

Abstract

Global temperatures are increasing, affecting timing and availability of vegetation along with relationships between plants and their consumers. We examined the effect of population density, herd body condition in the previous year, elevation, plant productivity and phenology, snow, and winter onset on juvenile body mass in 63 semi-domesticated populations of *Rangifer tarandus* throughout Norway using spatiotemporal generalized additive models (GAMs) and varying coefficient models (VCMs). Optimal climate windows were calculated at both the regional and national level using a novel nonlinear climate window algorithm optimized for prediction. Spatial and temporal variation in effects of population and environmental predictors were considered using a model including covariates decomposed into spatial, temporal, and residual components. The performance of this decomposed model was compared to spatiotemporal GAMs and VCMs. The decomposed model provided the best fit and lowest prediction errors. A positive effect of herd body condition in the previous year explained most of the deviance in calf body mass, followed by a more complex effect of population density. A negative effect of timing of spring and positive effect of winter onset on juvenile body mass suggested that a snow free season was positive for juvenile body mass growth. Our findings suggest early spring onset and later winter permanent snow cover as reinforcers of early-life conditions which support more robust reindeer populations. Our methodological improvements for climate window analyses and effect size measures for decomposed variables provide important contributions to account for, measure, and interpret nonlinear relationships between climate and animal populations at large scales.

Keywords Climate window · Decomposed covariates · Generalized additive models · Plant productivity · Reindeer · Varying coefficient models

Introduction

Climate change is strongly influencing the environment in the twenty first century (Sala et al. 2000), and average temperature increases are presently up to three times higher in the Arctic than elsewhere (Masson-Delmotte et al. 2018). This warming trend is leading to earlier spring events (Høye et al. 2007) and longer growing seasons (Keeling et al. 1996; Oberbauer et al. 2013), which can lead to a lack of synchrony between producer (e.g. plants) and consumer (e.g. herbivores) biological events. These trophic mismatches may negatively impact reproductive success and population recruitment in large herbivores (Post and Forchhammer 2008; Post et al. 2009). However, some herbivore populations have shown population growth as a result of milder weather conditions in the Arctic (Tyler et al. 2008). A clear understanding of plant-herbivore interactions under climate change is complicated by varied and lagged responses of vegetation to climate change. We examined one such relationship between climate, plant productivity and phenology, and a sub-Arctic herbivore in which evidence suggesting their success or failure under a changing climate has been

Communicated by Christian Kiffner.

✉ Hannah E. Correia
hcorreia@hsph.harvard.edu

[1] Harvard Data Science Initiative, Harvard University, Cambridge, MA, USA

[2] Department of Biostatistics, Harvard University, 655 Huntingdon Ave, Boston, MA 02115, USA

[3] Norwegian Institute for Nature Research (NINA), Fram Centre, Tromsø, Norway

[4] Department of Arctic and Marine Biology, The Arctic University of Norway, Tromsø, Norway

heavily mixed: the semi-domesticated reindeer, *Rangifer tarandus*.

Research on the effects of climate change on reindeer populations has focused on increased plant productivity and earlier phenology, along with winter conditions such as rain-on-snow events (Helle and Kojola 2008; Stien et al. 2012; Tveraa et al. 2013). Earlier onset of spring and low snow cover appear to benefit reindeer populations (Callaghan et al. 2011; Helle and Kojola 2008; Turunen et al. 2009), but increasing frequency of rapid winter warming events which create compacted snow and thick ice can limit reindeer's abilities to forage (Albon et al. 2016; Bokhorst et al. 2008; Hansen et al. 2011). Rain-on-snow events negatively impact reindeer fecundity (Stien et al. 2012) and survival (Hansen et al. 2019b). Further, deep snow pack increases energy expenditure of reindeer, reducing body condition over winter (Collins and Smith 1991; Helle and Kojola 2008), and forcing herds from higher elevation areas, which increases their susceptibility to predation (Tablado et al. 2014).

Autumn conditions, such as delayed onset of winter with later snowfall, and their potential importance to reindeer populations have largely been overlooked. Delayed onset of winter prompting decreases in autumn snow have the potential to counteract negative effects of harsher winters on reindeer populations (Loe et al. 2020; Movik 2018). However, warmer autumns from delayed winter onset can also affect herd nutrition via changes in plant phenology, with fitness consequences for females around the time of conception that influence juvenile mass and survival (Paoli et al. 2019, 2020; Veiberg et al. 2017). Juvenile herbivores are particularly sensitive to the effects of changing environmental conditions (Bonenfant et al. 2009; Gaillard et al. 1998; Ogutu et al. 2015; Owen-Smith 1990; Owen-Smith et al. 2005). Juvenile mass achieved at the onset of winter is density-dependent in many large ungulates, including reindeer (Sæther 1997; Skogland 1990), and is a main determining factor for winter survival of temperate and Arctic herbivore juveniles (Bonenfant et al. 2009; Gaillard et al. 1997), making it a key measure for reindeer population dynamics. We expect that insights on the role of autumn and early winter climate on reindeer populations through juvenile body mass is therefore key to establishing the consequences of climate change on Arctic herbivores.

Changes in climate, plant biomass, and phenology over time are not consistent across space, precipitating changes in herbivore populations that also vary over space (Gordon et al. 2004; Zhao et al. 2019). Thus, analyses of large-scale plant-herbivore systems require the incorporation of spatial information (Mårell et al. 2006; Ndegwa Mundia and Murayama 2009; Serneels and Lambin 2001). Generalized additive models (GAMs) and the related varying coefficient models (VCMs) are suitable for modelling spatial dependence (Hastie and Tibshirani 1990; Mu et al. 2018; Wood 2006), and both models have been employed extensively for spatial analyses in epidemiology, forestry, and large-scale fisheries management (Augustin et al. 2009, 2013; Finley 2011; Torabi 2014; Woolford et al. 2011). However, typical spatiotemporal GAMs and VCMs involve multidimensional nonparametric smoothing coefficient functions that are difficult to interpret. A modified GAM described by Oedekoven et al. (2017) used spatial and temporal averaging to create a more interpretable model, which has the potential to simplify incorporation of spatial and temporal effects. The model gives a practical approach for studying problems where it is desired to consider the average effects of spatial, temporal, and residual components separately. However, this model's prediction performance compared to the usual spatiotemporal GAM structure is unknown, the incorporation of interaction terms into the model has not been considered or explored, and the model's usability for ecologists and wildlife managers is not entirely clear. Nonparametric spatiotemporal models that accurately predict population responses, measure the spatial and temporal contributions of environmental variables to population changes, and capture large-scale vegetative transitions would be broadly applicable to ecologists studying the effects of climate change on vulnerable populations.

In this study, we extend and combine two statistical methods using nonparametric regression to model the relationship of vegetation and climate on the calf body mass of reindeer throughout Norway over three decades. We use this model to test our hypothesis that autumn and winter environmental conditions not typically examined in plant-herbivore systems, particularly the timing of the onset of winter, will have a moderate effect on juvenile reindeer body mass after accounting for spatiotemporal effects and density dependence. We accomplish this by (1) determining for specific climate variables which part of the year was most predictive of changes in individual juvenile condition of reindeer using a nonlinear climate window algorithm focused on prediction rather than model fit; (2) separately examining the spatial, temporal, and spatiotemporal associations of climate conditions and population characteristics to juvenile condition using a decomposed GAM with interaction terms; (3) assessing the prediction ability of the decomposed GAM with more common spatiotemporal GAMs through cross-validation; and (4) expanding inference for the variable decomposition approach by estimating effect sizes of the spatial, temporal, and spatiotemportal components for each decomposed variable and interaction variables separately, providing much-needed measures for interpretation of the decomposed model's results. We conclude by discussing the effects of spatial and temporal components of significant environmental predictors on juvenile reindeer body mass and the implications for relationships of plant productivity and phenology on sub-Arctic herbivores under climate change.

Methods

Reindeer data

The data on reindeer in Norway were collected from annual reports submitted by herders for 78 populations covering a majority of the Norwegian reindeer herding area (Tveraa et al. 2007), thereby providing consistent, long-term observations of ungulate responses to food availability across a large region. Reports from 1981–2015 included the estimated total number of reindeer in winter censuses and the average body mass in kilograms (±0.05 kg) of the slaughtered and skinned juveniles. Culling takes place in the first autumn of the calves' lives, between October and December (Marin et al. 2020). Five herds of domesticated reindeer in southern Norway were excluded (Lom, Vågå, Fram, and Filefjell), as they are managed differently from the Sami-managed semi-domesticated herds considered in our analyses; one more herd (district 30/31 Kautokeino vår-høstbeite) was removed for insufficient reporting due to reorganization of the herding districts. The average body mass of slaughtered calves for each herd was used as the response in all models. Two anomalous juvenile body mass observations were removed, where body mass was recorded as greater than 35 kilograms. Reindeer populations were grouped into ten management regions as in Tveraa et al. (2014).

Population size affects juvenile body mass, with larger populations resulting in lower juvenile body weights (Skogland 1990; Tveraa et al. 2013). Population density was therefore included as an area-adjusted predictor, calculated as a herd's population size divided by the area of that herd's summer pasture land in square kilometres. Since the mother's body condition before birth impacts her offspring's mass (Bårdsen and Tveraa 2012; Tveraa et al. 2003), we included maternal effects in modelling juvenile body mass by using the previous autumn/winter average juvenile slaughter weight as a measure of herd body condition previous to birth, as per Tveraa et al. (2014). Also, herd body condition in the previous year is also density dependent (Ballesteros et al. 2013; Bårdsen 2017), so an interaction between herd body condition and density was included in all models. Many of the study herds do not have access to pastures with favourable winter climate, and the relationship between food availability and herd condition differ between herds with access to favourable winter grazing lands and those without (Tveraa et al. 2007). Therefore spatial information and altitude are likely to contribute to variability in juvenile body mass. Longitude-latitude pairs representing approximate herd locations and the respective average elevation of the herd locations (obtained from normalized difference vegetation index (NDVI) data, see "Plant productivity" section) were included as predictors. There were insufficient observations of calf mass for years 1981–1983, 2014, and 2015, and since the previous year's calf mass was also used as a measure of herd body condition, the data used in all models were limited to years 1985–2013. Once matched to available climate data (see "Plant productivity" and "Climate and plant phenology" sections), 63 herding districts were represented in the analyses.

Plant productivity

Plant productivity was measured by the normalized difference vegetation index (NDVI) for locations within the herds' summer grazing land, data for which were collected by the Advanced Very High Resolution Radiometer (AVHRR) instrument deployed on a satellite system and available for full years since 1982 (Pinzon and Tucker 2014; Tucker et al. 2005). NDVI is calculated from visible red and near-infrared light reflected by vegetation. NDVI values range from zero to one, where NDVI values near zero indicate no visible plant productivity, when plant material has either died down or is covered by snowfall. We also obtained average altitudes of the areas from which NDVI values were taken. NDVI values were recorded twice a month, and the average NDVI value for all pixels (each pixel is 1 km^2) within a herd's summer pasture was calculated for each time point. In addition the average altitude, latitude, and longitude of the summer pastures were calculated for each herd using the GRASS GIS software (GRASS Development Team 2017).

Typically, NDVI values may be summarized over a month or season corresponding to ecologically significant grazing times for reindeer. The choice of period is highly dependent on assumptions about the importance of specific times of the year for reindeer, and the significance of these variables may depend entirely on how many NDVI values within a year are included in the summary statistic. Instead, we preferred to select the time of year and the window of time when plant productivity most strongly influenced reindeer health, i.e., body mass. We devised an improved method based on a technique by van de Pol et al. (2016) using flexible, non-parametric GAMs to determine the optimal window with highest prediction power for each environmental variable (Staton et al. 2017).

While red and infrared light values to calculate NDVI are recorded year-round, NDVI values for the parts of Norway located within the Arctic Circle during the winter months with polar nights are not meaningful, since satellites are unable to obtain accurate visible light readings. The reindeer in the Finnmark region of Norway have common winter pastures in the interior (Tveraa et al. 2013, 2014), however the populations further south remain in their pasture locations year-round. Annual cullings take place between September

and March each year, however exact dates for herd cullings are not recorded. Therefore, we considered only those NDVI values from mid-April (week 15) to mid-October (week 43) when reindeer calves were most likely to be occupying the summer pastures and NDVI values were expected be greater than zero. Suitable NDVI windows for each of 10 herding regions as defined in Tveraa et al. (2014) and one window for all of Norway were determined by selecting a predictive time window for each region, as described below. The same approach was used for calculating a national window for NDVI.

Since the relationship between NDVI and reindeer body mass could be nonlinear and the form of the relationship is unknown, a GAM of the form

$$\mathbb{E}(Y) = \beta_0 + f(x)$$

was used to determine the forecasting performance of various windows for NDVI, assuming a Gaussian distribution, β_0 as the parametric intercept, juvenile body mass as the response Y, the mean NDVI calculated for a given window as the predictor x, and f as the unknown smooth function relating yearly mean NDVI to juvenile body mass. For each year, the response of juvenile body mass was averaged over space within regions when calculating the regional windows and averaged over the entire country for the national window. Less than one-third of the total Sami herds submitted annual reports for years before 1984, and this would skew the national average of juvenile body mass for those years. Therefore, only NDVI and herd data from 1984 to 2013 were used for all windows. A mean absolute error (MAE) was calculated for each window using a time-series forecast cross-validation procedure, with a minimum of 10 years of data (from 1984 to 1993) used to train the model (Staton et al. 2017). Since the raw NDVI values were summarized for every two weeks, we set the minimum window size to four weeks to provide at least two NDVI values to be averaged. This prevented late snow melts from creating a mean NDVI of zero. Zero values contributed no information for the model. We therefore limited the window searches to the Julian weeks of 15–42 for the national climate window, while the search windows for each region were limited to weeks 22–39 (typically the beginning of June to end of September), due to several northern regions having short snow-free summers. The mean NDVI using the regional window (indicated by $\text{rNDVI}_{\mathbf{s},t}$, where, henceforth, each location of a herd's summer pasture is $\mathbf{s} \in S$ where S is the set of locations with longitude-latitude coordinates u, v, and t is the year) was calculated for each year from 1985 through 2013 at each herd's location using the optimal window for NDVI for that herd's respective region. The mean NDVI using the national window (indicated by $\text{nNDVI}_{\mathbf{s},t}$) was also calculated for each year at each herd's location. Regional differences in span and the beginning and end points of windows were compared to the national window.

Climate and plant phenology

Since maximum increase in vegetation is positively associated with high quality forage (Hamel et al. 2009), availability of high-quality forage for reindeer was measured by the day of the year (DOY) when the maximum NDVI value first occurred for each herd's location and each year. Spring onset for each year and each herd's location was considered as the DOY when NDVI first reached 50% of its yearly maximum. This was formally defined as the first DOY when the value of NDVI was equal to $[\max(\text{NDVI}) - \min(\text{NDVI})]/2$, where max(NDVI) was the maximum NDVI value for a given herd's location in a given year and min(NDVI) was the minimum NDVI value for the same location in the same year (Tveraa et al. 2013). Since red and infrared light from vegetation are very low in winter months due to significant snow cover, even in areas without polar nights, min(NDVI) is almost always equal to 0. The date at which NDVI values reached 50% of their yearly maximum is a good approximation of peak vegetative green-up and maximum nitrogen concentration in forage plants in Arctic regions (Doiron et al. 2013; Hogrefe et al. 2017). Both the DOY when maximum NDVI occurred and spring onset were calculated from the AVHRR data (Pinzon and Tucker 2014; Tucker et al. 2005). Daily snow depth (mm) for each of the herding districts from 1984 to 2013 were obtained from the Norwegian Meteorological Institute (Lussana et al. 2018; MET Norway 2018). The area under the spline curve (AUC) of ground snow depth was calculated for each year at the summer grazing pastures using daily snow depth values from September to September. To capture the beginning of continuous snow cover for the winter season of a given year, the onset of winter for a given year was defined as the first DOY which had at least two consecutive weeks of snow on the ground (snow depth > 0 mm). These two variables captured the severity and duration of the snow cover season, since increased snow depth and snow cover duration can reduce the physical condition of reindeer, affect soil moisture and nutrient levels, and change plant phenology (Helle and Kojola 2008; Tomaszewska et al. 2020).

GAMs and VCMs

To model juvenile reindeer body mass, we considered a generalized additive model with interaction (Coull et al. 2001). In order to include spatiotemporal information appropriately, we used the model

$$\mathbb{E}(Y) = F_{\mathbf{s},t} + f_5(\text{NDVI}_{\mathbf{s},t}) + G^G_{\mathbf{s},t}\,, \tag{1}$$

where

$$F_{\mathbf{s},t} = z_0(\mathbf{s},t) + f_{v_{\text{cat}}}(\text{elev}_{\mathbf{s}}) + f_1(\text{peakNDVIdoy}_{\mathbf{s},t}) + f_2(\text{SOdoy}_{\mathbf{s},t}) + f_3(\text{WPGSdoy}_{\mathbf{s},t}) + f_4(\text{B}_{\mathbf{s},t-1}, \text{N}_{\mathbf{s},t})$$

and

$$G^G_{\mathbf{s},t} = f_6(\text{B}_{\mathbf{s},t-1}) + f_7(\text{N}_{\mathbf{s},t}) + f_8(\text{snow}_{\mathbf{s},t}) \, .$$

Here, $\text{elev}_{\mathbf{s}}$ was the average elevation of the herd's summer grazing lands, $\text{B}_{\mathbf{s},t-1}$ was herd body condition in the previous year, $\text{N}_{\mathbf{s},t}$ was population density of the herd, $(\text{B}_{\mathbf{s},t-1}, \text{N}_{\mathbf{s},t})$ was the tensor product interaction of herd condition in the previous year with herd population density in the observed year, $\text{NDVI}_{\mathbf{s},t}$ was the mean NDVI of the predetermined window (one of rNDVI or nNDVI), $\text{peakNDVIdoy}_{\mathbf{s},t}$ was the DOY when peak NDVI occurred, $\text{SOdoy}_{\mathbf{s},t}$ was spring onset, $\text{snow}_{\mathbf{s},t}$ was the AUC of snow, and $\text{WPGSdoy}_{\mathbf{s},t}$ was the onset of winter. The spatiotemporal component was accommodated via a three-dimensional tensor smoothing function z_0, while $f_1, \ldots, f_8$ represent one-dimensional smoothers. The response $\mathbb{E}(Y)$ is average juvenile body mass assuming a scaled Student's t distribution, $(Y - \mu)/\sigma \sim t_\nu$, where σ and ν are estimated alongside the smoothing parameters (Wood et al. 2016). The Student's t distribution was preferred, since the average juvenile body mass was a heavy-tailed response variable. To ensure the effects of latitude on elevation were removed, elevation was categorized into three groups by latitude in kilometres from 0° latitude: south (<7200 km), mid (7200–7600 km), and north (>7600 km). The term $f_{v_{\text{cat}}}(\text{elev}_{\mathbf{s}})$ generated a different smooth for each latitudinal category of elevation, where v_{cat} is the latitude categories south, mid, and north. The R (version 4.0.3) package **mgcv** was again used to fit the GAM using the regional climate windows for NDVI,

$$\mathbb{E}(Y) = F_{\mathbf{s},t} + f_5(\text{rNDVI}_{\mathbf{s},t}) + G^G_{\mathbf{s},t} \, ,$$

henceforth labeled as GAMr, and the GAM using the national climate window for NDVI,

$$\mathbb{E}(Y) = F_{\mathbf{s},t} + f_5(\text{nNDVI}_{\mathbf{s},t}) + G^G_{\mathbf{s},t} \, ,$$

henceforth GAMn, and estimate their parameters (R Core Team 2020; Wood 2017).

VCMs, which are related to GAMs, were also considered in our analyses for their ability to include covariate spatiotemporal effects in the model. Herd body condition in the previous year and population density are likely to be spatially-dependent, as northern herds are on average denser than southern herds in Norway (Tveraa et al. 2013). NDVI and snow depth are also spatially-dependent, with northern and inland locations generally having shorter growing season, lower NDVI values, and more snow than southern and coastal locations (Pettorelli et al. 2005; Hogda et al. 2001; Dyrrdal et al. 2013). Tensor product smooths have been used with success in fisheries and ecology research to handle environmental covariates where the effect is expected to change over space and time (Augustin et al. 2013; Finley 2011; Phillips et al. 2014). We employ a partial VCM given as

$$\mathbb{E}(Y) = z_0(\mathbf{s},t) + \sum_{k=1}^{p} f_k(x_k) + \sum_{j=1}^{q} z_j(\mathbf{s},t) \cdot w_j \, , \tag{2}$$

where x_k are predictors that are not considered spatially dependent, f_k are unknown smooth functions, w_j are spatially-varying predictors for specific locations and time points, and z_0, z_j are unknown tensor product smooths constructed using three-dimensional spatiotemporal basis functions that account for the differing units of measure in space and time. The partial VCM structure allows for functional coefficients of four predictor variables (herd body condition, population density, NDVI, and snow depth) to vary over space and time. We can rewrite (2) in the explicit notation of (1) as

$$\mathbb{E}(Y) = F_{\mathbf{s},t} + f_5(\text{NDVI}_{\mathbf{s},t}) + G^V_{\mathbf{s},t} \, , \quad \text{where}$$

$$G^V_{\mathbf{s},t} = z_1(\mathbf{s},t) \cdot \text{B}_{\mathbf{s},t-1} + z_2(\mathbf{s},t) \cdot \text{N}_{\mathbf{s},t} + z_3(\mathbf{s},t) \cdot \text{NDVI}_{\mathbf{s},t} + z_4(\mathbf{s},t) \cdot \text{snow}_{\mathbf{s},t} \, ,$$

and $F_{\mathbf{s},t}$ is as defined previously. The partial VCM denoted VCMr that includes the regional NDVI window, defined as

$$\mathbb{E}(Y) = F_{\mathbf{s},t} + f_5(\text{rNDVI}_{\mathbf{s},t}) + G^V_{\mathbf{s},t} \, ,$$

and the VCM denoted VCMn with the national NDVI window, given as

$$\mathbb{E}(Y) = F_{\mathbf{s},t} + f_5(\text{nNDVI}_{\mathbf{s},t}) + G^V_{\mathbf{s},t} \, ,$$

were also fit using the **mgcv** package in R version 4.0.3 (Hastie and Tibshirani 1993; Wood 2017).

Decomposed interactions model

We wished to examine spatial and temporal components for eight of the variables in (1): herd body condition in the previous year, population density, the interaction of herd condition in the previous year with population density, mean NDVI, peak NDVI DOY, spring onset, AUC of snow depth, and onset of winter. We employed a technique where each variable was decomposed into spatial, temporal, and residual components by averaging over time and over space (Oedekoven et al. 2017). Specifically, given a variable $Q_{\mathbf{s},t}$ with a value at each location $\mathbf{s} \in S$ where S is a collection of locations represented as longitude-latitude pairs u, v and time $t = 1, \ldots, T$, the spatial component of variable Q is represented by the average of Q over time for each location, and the temporal component of Q is the average of Q over space for each time point,

$$Q_{\mathbf{s}} = \frac{1}{N_T}\sum_{t=1}^{T} Q_{\mathbf{s},t} \qquad \text{and} \qquad Q_t = \frac{1}{N_S}\sum_{\mathbf{s}\in S} Q_{\mathbf{s},t}$$

respectively, where N_T is the number of time points for each location and N_S is the number of spatial points or locations for each time point. The residual component is calculated by subtracting from the original value of $Q_{\mathbf{s},t}$ the spatial and temporal components, $Q_r = Q_{\mathbf{s},t} - Q_{\mathbf{s}} - Q_t$.

The decomposed model we chose to compare to the GAMs and partial VCMs given in the "GAMs and VCMs" section was

$$\begin{aligned}\mathbb{E}(Y) =& f_{v_{\text{cat}}}(\text{elev}_{\mathbf{s}}) + f_1(\text{B}_{\mathbf{s}}) + f_2(\text{B}_{t-1}) + f_3(\text{B}_r) + f_4(\text{N}_{\mathbf{s}}) + f_5(\text{N}_t) + f_6(\text{N}_r)\\ &+ f_7(\text{B}_{\mathbf{s}}, \text{N}_{\mathbf{s}}) + f_8(\text{B}_{t-1}, \text{N}_t) + f_9(\text{B}_r, \text{N}_r)\\ &+ f_{10}(\text{nNDVI}_{\mathbf{s}}) + f_{11}(\text{nNDVI}_t) + f_{12}(\text{nNDVI}_r)\\ &+ f_{13}(\text{peakNDVIdoy}_{\mathbf{s}}) + f_{14}(\text{peakNDVIdoy}_t)\\ &+ f_{15}(\text{peakNDVIdoy}_r)\\ &+ f_{16}(\text{SOdoy}_{\mathbf{s}}) + f_{17}(\text{SOdoy}_t) + f_{18}(\text{SOdoy}_r)\\ &+ f_{19}(\text{snow}_{\mathbf{s}}) + f_{20}(\text{snow}_t) + f_{21}(\text{snow}_r)\\ &+ f_{22}(\text{WPGSdoy}_{\mathbf{s}}) + f_{23}(\text{WPGSdoy}_t) + f_{24}(\text{WPGSdoy}_r)\ ,\end{aligned}$$

where all variables are decomposed versions of those given in (1) and nNDVI being the mean of NDVI for the country-wide window selected in the "Plant productivity" section. The national window for NDVI was essential to enable spatial and temporal decomposition of the effect of mean NDVI calculated from a standardized, country-level window. While the covariate smoothers discussed in the "GAMs and VCMs" section attempt to account for spatial and spatiotemporal effects by smoothing the variable over space-time, decomposing the variables into spatial, temporal, and residual components allows us to consider their average effects separately. A significant extension of the Oedekoven et al. (2017) decomposition in this study is the inclusion of decomposed interaction terms $f_7(\text{B}_{\mathbf{s}}, \text{N}_{\mathbf{s}})$, $f_8(\text{B}_{t-1}, \text{N}_t)$, and $f_9(\text{B}_r, \text{N}_r)$ into the decomposed model, which has not been considered previously. These terms specifically allow us to examine the interaction of the spatial, temporal, and residual components of herd body condition and herd density. We therefore refer to this model as the decomposed interactions model, henceforth denoted DIMn.

Proportion of deviance explained

We quantified the contribution of each predictor to the complete model by calculating the proportion of deviance explained for each variable,

$$D_p = \frac{D_{red} - D_{full}}{D_{null}},$$

where D_{full} is the deviance of the full model, D_{red} is the deviance of the reduced model with the variable of interest removed, and D_{null} is the deviance of the null model. Typically, the scaled Student's t distribution parameters ν and σ can be estimated automatically when fitting a GAM with such a distribution in **mgcv**. Care must be taken to use identical values for parameters ν and σ for the full, reduced, and null models when calculating proportion of deviance explained for GAMs and partial VCMs using the scaled Student's t distribution. We chose to allow **mgcv** to estimate the distribution parameters for the full decomposed interactions model, then used these same parameters when fitting the reduced and null models. Deviance explained was calculated for each of the decomposed variables in the DIMn model and their undecomposed counterparts in the GAMr model for direct comparison of the predictors in each model.

Cross-validation and model comparison

GAM and partial VCM variations (see "GAMs and VCMs" section) were considered to determine an optimal model through both fit and prediction. We wished to ascertain if a national window for NDVI was sufficient for accurate prediction of juvenile reindeer body mass, or whether windows that maintain regional differences in NDVI were more accurate descriptions. Additionally, we wanted to compare the prediction capabilities of the decomposed interactions model with known modelling techniques that account for spatiotemporal autocorrelation. Since overfitting is a concern for the decomposed model (Oedekoven et al. 2017), cross-validation was also used to determine whether overfitting was a problem for Equation (3). If so, the decomposed interactions model would have much larger prediction errors than the model VCMn that includes spatiotemporal smoothers for herd body condition, population density, the herd condition and density

interaction, NDVI averaged using the national window, and AUC of snow depth. The prediction accuracies of the models were compared using random 10-fold cross validation (CV) and 10-fold CV for grouped data. In the random 10-fold CV, observations were randomly assigned to one of 10 folds. In the 10-fold CV for grouped data (which will be referred to as herd 10-fold CV), observations grouped by herd location were randomly selected to a specific fold. This allowed us to establish how well the model could predict at new spatial locations (Roberts et al. 2017). To estimate the CV prediction error we used nine of the 10 folds as training datasets and the remaining fold as a testing dataset. We then calculated the median absolute deviations for each $k \in \{1, 2, \ldots, 10\}$ fold, MAD_k, and summarized the fold-based errors as $\mathbf{M}_{\mathrm{CVE}} = \mathit{median}(\mathrm{MAD}_1, \mathrm{MAD}_2, \ldots, \mathrm{MAD}_{10})$.

The Kruskal-Wallis rank sum test was used to determine if the $\mathbf{M}_{\mathrm{CVE}}$ varied significantly among all the tested models for each CV procedure. If significant differences were detected, pairwise comparisons using the Wilcoxon signed rank test with Bonferroni corrections for multiple testing were employed to assess whether the decomposed interactions model was significantly better than other models at accurately predicting out-of-sample values. If significant differences were not detected by the Kruskal-Wallis rank sum test, adjusted R^2 values and Akaike's Information Criteria (AIC) were compared to evaluate the model fit. The model with lowest $\mathbf{M}_{\mathrm{CVE}}$ across all CV procedures, highest adjusted R^2, and lowest AIC was preferred. Finally, restricted maximum likelihood (REML) estimation was used for calculation of smooth term p-values in the preferred model instead of the default generalized cross-validation (GCV) in **mgcv**, because REML estimation is less prone to undersmoothing (Wood 2017).

Results

Most regions had diverse window sizes and optimal weeks of the year for NDVI, with a general trend of windows moving from the first half of the NDVI curve to the second half while progressing from northeast Norway to southern Norway through the herding regions. The estimated optimal window for NDVI to predict the national average of juvenile body mass was for weeks 27 through 42, which overlapped many regional optimal windows for NDVI (SI Fig. S2).

Four GAM and partial VCM variations and the decomposed interactions model were evaluated for prediction accuracy using random 10-fold and herd 10-fold CV procedures. Adding spatiotemporal smooths to NDVI, snow depth, herd condition in the previous year, and population density generally improved fit, however prediction for VCMr and VCMn did not improve substantially for either CV procedures (Table 1). Models that included NDVI calculated using national windows provided better prediction and comparable fit to models with NDVI calculated using the regional window. The DIMn model had the best fit and lowest prediction errors. Differences in $\mathbf{M}_{\mathrm{CVE}}$ among the five models for the herd 10-fold CV procedure were apparent ($p < 0.05$), but no differences among those models for the random 10-fold CV procedure were revealed (Table 1). The DIMn model was better than the VCMr ($p = 0.039$) and VCMn ($p = 0.008$) models for predicting out-of-sample-values in the herd 10-fold CV procedure. It should be noted that GAMs and VCMs are known to lose prediction accuracy when smooth variables have a range outside of the training dataset, as evidenced by the increasing $\mathbf{M}_{\mathrm{CVE}}$ from random 10-fold CV to herd 10-fold CV for most of the models (Table 1).

Table 1 Median absolute cross-validation prediction errors ($\mathbf{M}_{\mathrm{CVE}}$), adjusted R^2, and Akaike's Information Criteria (AIC) values for each of four variations of either generalized additive models (GAMr and GAMn) or varying coefficient models (VCMr and VCMn) and the decomposed interactions model (DIMn). *P* values for the Kruskal–Wallis rank sum test with degrees of freedom = 4 are also given for each of the two cross-validations

Model	Random 10-fold $\mathbf{M}_{\mathrm{CVE}}$	Herd 10-fold $\mathbf{M}_{\mathrm{CVE}}$	adj. R^2	AIC
GAMr	0.953	1.057	0.638	5895.837
GAMn	0.897	1.029	0.638	5889.638
VCMr	0.903	1.052	0.645	5858.642
VCMn	0.896	1.026	0.646	5841.539
DIMn	0.868	0.829	0.685	5608.885
Kruskal–Wallis *P* value	0.324	0.040		

The decomposed interactions model was fit for inference and compared to the fit of GAMn (see SI "Fit of the GAMn model" section). The component smooth functions of GAMn highlighted the nonlinear relationships between many of the predictors and juvenile body mass (SI Fig. S3). However, the spatial, temporal, and residual components of predictor variables in DIMn were often substantially different from their singular smooth versions in GAMn (Figs. 1 and 2). The spatial component of herd condition ($\mathrm{B_s}$), i.e. the herd's body condition averaged over time, was linear and positively related to juvenile body mass (Fig. 1). This was expected, as herd body condition was represented as the previous year's juvenile body mass. As in GAMn, the interaction between the temporal components of herd condition and population density and the interaction between the residual components of herd condition and population density in DIMn were significant, so the individual variables are not directly interpretable. For the interaction between the temporal components of herd condition in the previous year and population density ($\mathrm{B}_{t-1}, \mathrm{N}_t$), low herd condition

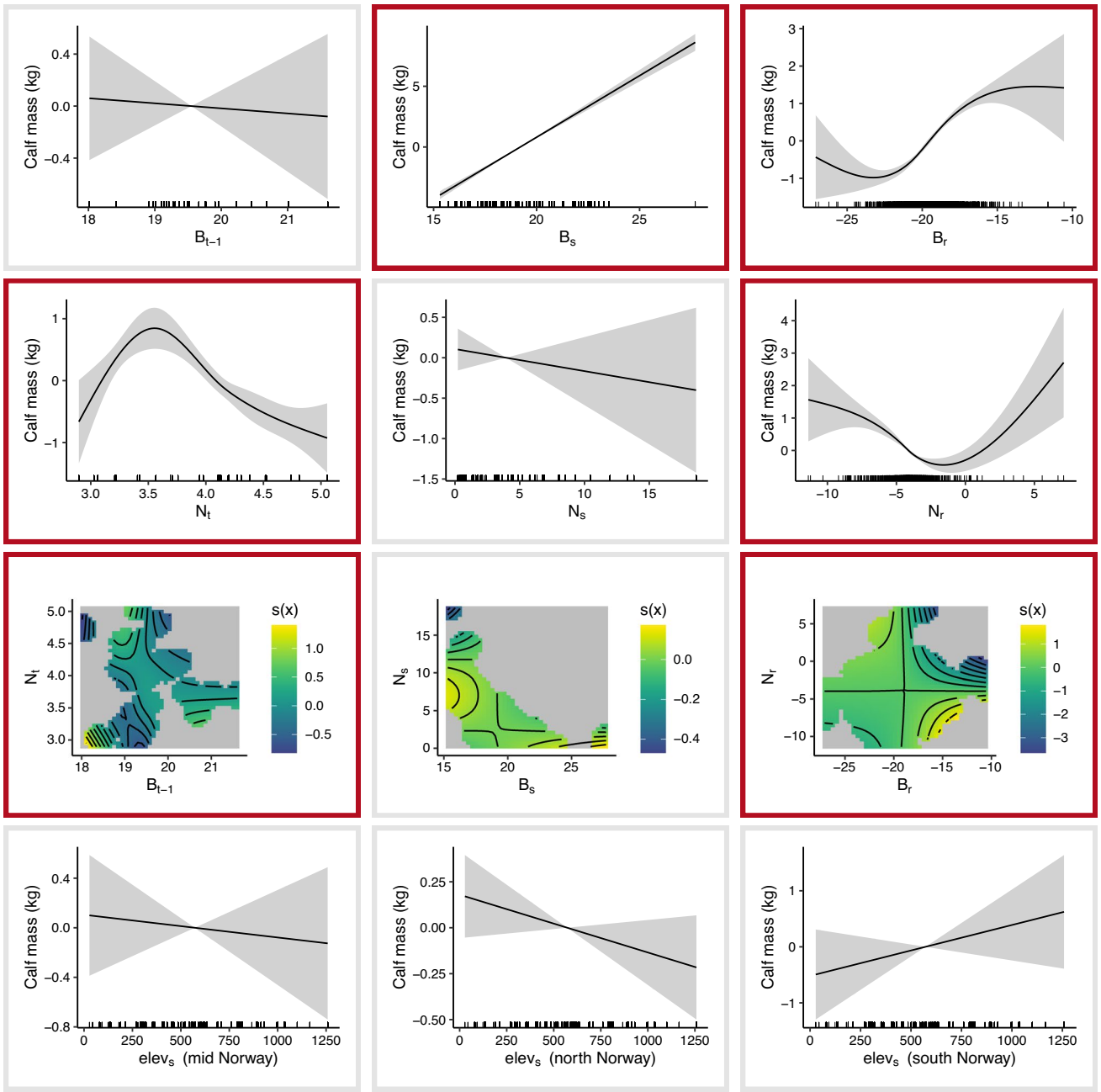

Fig. 1 Temporal, spatial, and residual component smooth functions of reindeer and elevation predictors in decomposed interactions model (DIMn). Smooth terms with $p < 0.05$ are bordered in red. Top row: herd body condition in the previous year (B); second row: population density (N); third row: interaction between herd condition in previous year and population density (B, N); fourth row: elevation categorized by latitude ($elev_s$)

combined with low densities was associated with an increase to juvenile body mass over time (Fig. 1, third row, far left). For the interaction of the residual herd condition and density components (B_r, N_r), lower B_r values that corresponded to herd condition values being smaller than the spatial and temporal averages, combined with N_r values between −4 and 5 that occur when herds with population densities were close to the sum of its temporal and spatial components, coincided with lower calf body mass (Fig. 1, third row, far right). Years with peak NDVI DOY ($peakNDVIdoy_t$) occurring later corresponded to increasing juvenile body mass, while years with later spring onset ($SOdoy_t$) or high NDVI values ($nNDVI_t$) had lower calf masses (Fig. 2). Years with later winter onset ($WPGSdoy_t$) also coincided with heavier juveniles. The residual spatiotemporal component of winter onset ($WPGSdoy_r$) was positively linearly associated with

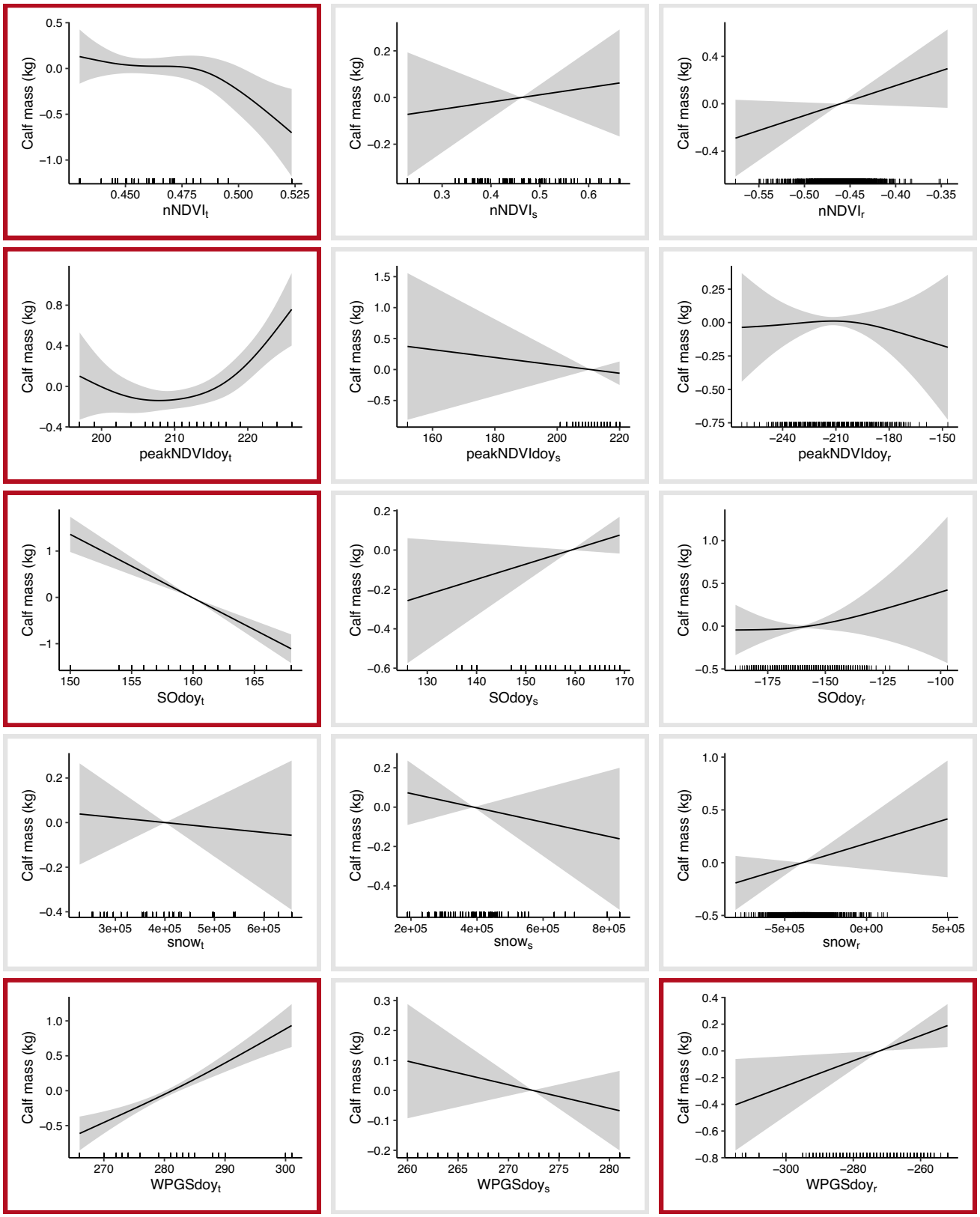

Fig. 2 Temporal, spatial, and residual component smooth functions of environmental predictors in decomposed interactions model (DIMn). Smooth terms with $p < 0.05$ are bordered in red. Top row: mean normalized difference vegetation index as calculated using the national window (nNDVI); second row: peak NDVI day of the year (peakNDVIdoy); third row: spring onset day of the year (SOdoy); fourth row: snow area under the curve (snow); fifth row: winter permanent ground snow day of the year (WPGSdoy)

Table 2 Proportion of deviance explained for variables in the generalized additive model using nationally-summarized normalized difference vegetation index (NDVI), labeled GAMn, and decomposed interactions model (DIMn). For DIMn, the proportion of deviance explained is broken down into spatial, temporal, and residual components as well as providing the total proportion of deviance explained for each variable

Variable	GAMn	DIMn			
		Temporal	Spatial	Residual	Total
s, *t*	0.08	–	–	–	–
Herd body condition in prev. yr. (B)	0.11	0.00	0.33	0.18	0.50
Population density (N)	0.09	0.02	0.00	0.04	0.06
Interaction of herd condition in prev. yr. and population density (B, N)	0.01	0.03	0.00	0.01	0.05
Elevation (elev)	0.06	–	–	–	0.00
Mean NDVI from national window (nNDVI)	0.01	0.01	0.00	0.00	0.01
Peak NDVI day of the year (peakNDVIdoy)	0.00	0.01	0.00	0.00	0.01
Spring onset day of the year (SOdoy)	0.00	0.03	0.00	0.00	0.03
Snow area under the curve (snow)	0.00	0.00	0.00	0.00	0.00
Winter permanent ground snow day of the year (WPGSdoy)	0.01	0.03	0.00	0.00	0.03

juvenile body mass, namely, true winter onset values earlier than the spatial and temporal averages, resulting in lower $WPGSdoy_r$ values, corresponded to lower-than-average calf masses.

The proportion of deviance explained for each of the variables in GAMn and their decomposed components in DIMn was often small (Table 2). Herd condition in the previous year explained the largest proportion of deviance in both GAMn and DIMn, followed by population density in both models. Elevation explained 6% of the deviance in GAMn but did not explain any variation in DIMn. When broken down into decomposed components, the largest proportion of deviance in DIMn was explained by the spatial component of herd condition, followed by the spatiotemporal residual component of herd condition. The spatiotemporal residual component of population density explained 4% of the deviance in the decomposed interactions model, while 3% of the deviance was each explained by the interaction of the temporal components of herd condition and population density, along with the temporal components of winter permanent ground snow DOY and spring onset DOY.

Interactions between the decomposed components of herd body condition and population density on the predicted average juvenile body mass from DIMn were further broken down in Fig. 3 and SI Figs. S4 to S6. Predicted calf mass strongly resembled the temporal component of herd body condition, since the latter was just average calf mass lagged by one year (Fig. 3a). Additionally, above average herd body condition and predicted calf mass were preceded or accompanied by lower-than-average population densities. Over space, herds with consistently high population densities and low herd body condition corresponded with persistently low weight calves and were concentrated in northern Norway (Fig. 3b). Herds with consistently low densities and mid to high herd conditions tended to have more stable juvenile body weights. Herds with years when true herd condition values larger than the spatial and temporal averages, resulting in greater B_r values, typically occurred in the southern half of Norway (SI Fig. S4). The exceptions were during the 1994–1995 and 2002–2004 periods, when the spatially-averaged B_{t-1} component was much larger than the overall average (Fig. 3a). Herds in the northern half of Norway typically had greater values for N_r generated by true population densities being higher than the spatial and temporal averages (SI Fig. S5). However, the period of 1996–2003 for that region had true population densities equal to or less than the N_t and N_s components, when there was a dip in spatially-averaged population densities (Fig. 3a). These spatial and temporal variations in herd body condition and density resulted in predicted average juvenile body mass from the DIMn ranging from 15 to 26 kg, with herds located in southern regions of Norway typically having heavier calves than northern herds (SI Fig. S6).

Discussion

We used nonparametric regression to determine the optimal regional and national NDVI windows that best predict average juvenile reindeer body mass, along with other relevant herd, environmental, and plant phenology predictors and assessed various model structures for fit, prediction, and interpretability of spatiotemporal data. NDVI summarized using the national window describes and predicts changes in average juvenile body mass for individual herds as adequately as NDVI averaged using the regional windows. The three-dimensional spatiotemporal smooth included in the GAMs and VCMs captures the variation between herds not captured by the climate and vegetation variables in these models, acting as a nuisance variable. The relationships found among the climate and vegetation variables and calf mass are thus independent of location and year (e.g., for a

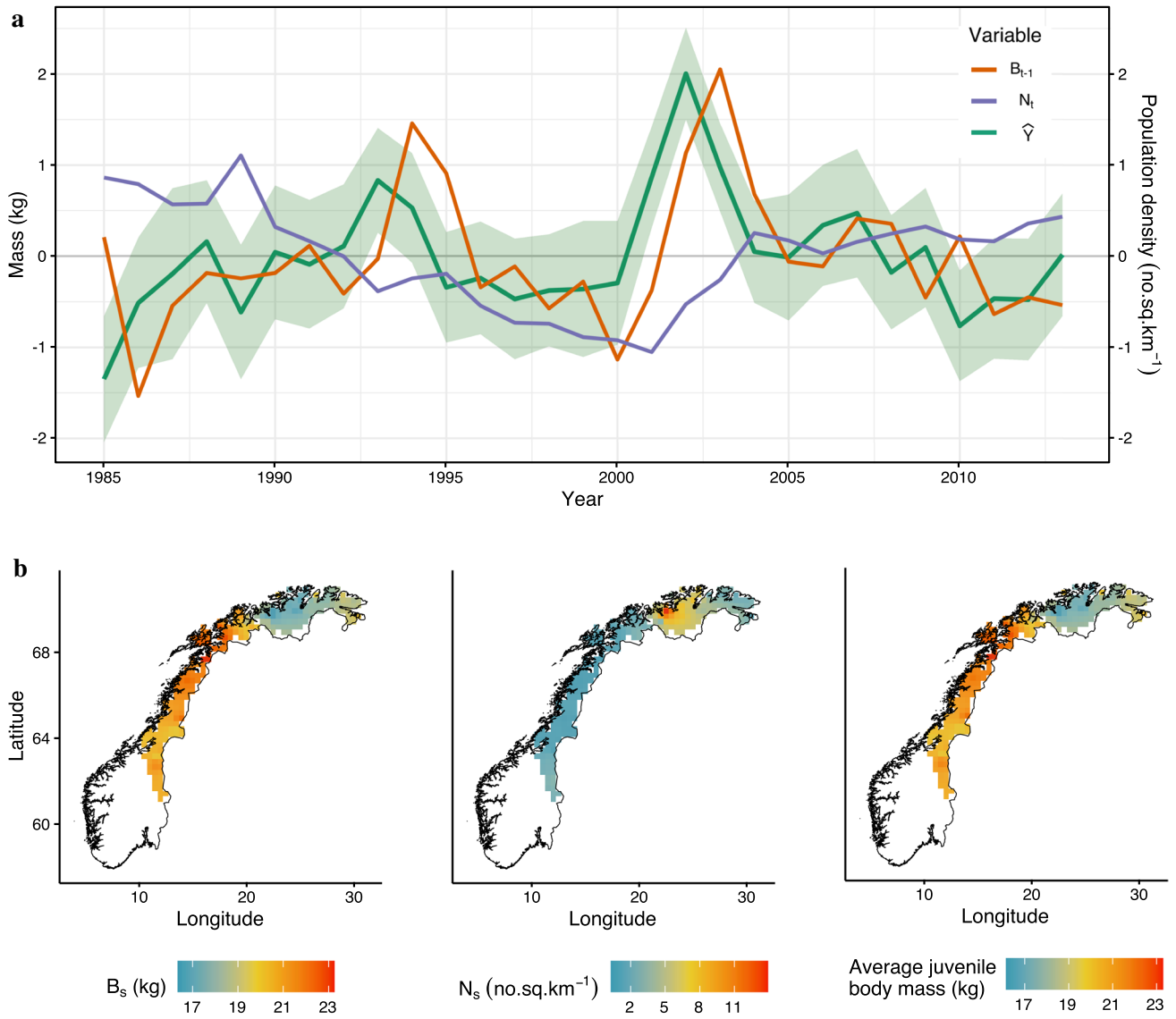

Fig. 3 Interactions of spatial components and temporal components from the decomposed interactions model (DIMn) on average juvenile reindeer body mass. **a** Centred temporal components of herd body condition in the previous year (B_{t-1}, dark orange) and population density (N_t, purple) overlaid on the centred predicted average juvenile body mass from the DIMn model ($\hat{Y}$, green) for years 1985–2013. Approximate pointwise 95% confidence intervals for $\hat{Y}$ are shaded in green. **b** Spatial components of herd body condition in the previous year (B_s, left) and population density (N_s, centre) and the predicted average juvenile body mass from the DIMn model averaged over time ($\hat{Y}$, right)

given herd, population density has a nonlinear relationship to average calf body mass). Therefore, the effects of climate and vegetation shown in our results are average effects for any reindeer calf within the spatial range of the data used in our analyses. Accounting for spatiotemporal variation in several of the predictors only improves prediction for locations within the range of the training data, a well-known limitation of GAMs and VCMs due to the way basis functions are constructed (Moisen and Frescino 2002). The decomposed interactions model produces the best fit and lowest cross-validation prediction errors, and the ability to calculate proportional deviances for spatial, temporal, and residual components of each variable increases the interpretability of such a model.

While complex smoothers can improve fit and prediction by accounting for spatiotemporal correlations in data, a disadvantage of GAMs and VCMs with complex smoothers is that they are difficult to interpret. Effects of smoothed variables over two or three dimensions become difficult to ascertain. While hotspots and low points can be visualized using three-dimensional smoothers over space-time, the size of the direct effect is difficult to quantify. We have shown

that the decomposed model structure of Oedekoven et al. (2017) allows the effect of a covariate to be more easily measured over space and time separately while still producing an effective model for prediction. Further, we have illustrated the incorporation of interaction terms into the decomposed model and provided detailed interpretation of their use and inference. Moreover, we have devised a simple way to quantify the contribution of the components of the model, which allows researchers to determine whether spatial or temporal effects are more pronounced for each decomposed variable of interest.

The change in NDVI seen in the Norwegian reindeer herds' summer locations and observed in similar boreal regions Park et al. (2016) is likely to have effects on juvenile growth rates and consequences for over-winter survival. The NDVI window that best predicted the national mean of juvenile body mass was from the beginning of July to the first week of October, reflecting the relationship between high-quality food and juveniles body mass. Calving for Norwegian reindeer occurs in May to early June (Reimers 2002; Holand et al. 2003), and calves are capable of eating solid food within a month after birth. Juveniles are therefore likely to be consuming large volumes of high-quality forage in addition to their mothers' milk soon after birth in order to quickly put on mass before the arrival of winter in late October. Observed changes in calving dates of reindeer in the Arctic Circle indicate plastic responses of females to milder fall and winter conditions (Paoli et al. 2018), which will likely expand the time in which calves and reproducing females can feed on high-nutrition plant material and put on mass before winter. These responses may be necessary if reindeer populations are to avoid widespread starvation and population collapse during winter warming events that have been observed with increasing frequency in the Arctic (Aanes et al. 2002; Albon et al. 2016).

Lack of availability to varied elevation may alter reindeer responses to extended spring and summer seasons, however. In the south, lower elevation corresponded to below-average calf mass. Southern reindeer herds experienced persistently low juvenile body masses, perhaps related to reduced grazing activity from prolonged insect harassment common at low elevations (Colman et al. 2003; Vistnes et al. 2008; Weladji et al. 2003), as these reindeer remain on the same grazing pastures year-round and do not have access to higher elevations. As warmer seasons become longer, reindeer in southern Norway may be unable to compensate for such prolonged stress (Colman et al. 2003). In cooler regions where insect harassment is less severe or prolonged and some herd migration is common, semi-domesticated reindeer exhibited more nuanced preferences for elevation likely driven by food availability, protection against predators, and avoidance of human activity common to their wild counterparts (Pape and Löffler 2015; Vistnes et al. 2008).

The interplay between population density, herd body condition, and calf weight in reindeer is complex. A mother's weight significantly influences her calf's weight, and both adult and juvenile body weights are negatively related to herd density (Bårdsen and Tveraa 2012; Tveraa et al. 2003, 2013). The expected density-dependence of juvenile body mass and interactions between herd body condition and density were apparent for herds in our analyses (Bårdsen 2017; Tveraa et al. 2003). Presumed positive effects of increased plant productivity on juvenile body mass may be unlikely to overcome maternal effects and intrapopulation competition for food during the early and late weeks of the growing season, where availability of edible vegetation are more limited (Veiberg et al. 2017). This is reinforced by the higher proportions of deviance explained for herd condition in the previous year and population density predictors compared to those for NDVI and peak NDVI DOY. An extended growing season and overall warming of the Arctic ecosystem (Masson-Delmotte et al. 2018; Oberbauer et al. 2013) has contrasting effects on reindeer. On the one hand, earlier vegetative onset in the spring increased calf weight and survival, likely through both mother and calf access to high-quality forage (Bårdsen and Tveraa 2012; Tveraa et al. 2013). However, warmer autumn and winter temperatures delay or compress the mushroom fruiting season, affect distribution of spores, and change mushroom abundance in Fennoscandia, an important food source for reindeer during the autumn, which may contribute to reduced female herd condition and consequently female reproductive success (Collado et al. 2019; Kauserud et al. 2008, 2010, 2011; Paoli et al. 2019). Therefore, earlier spring onset and later permanent ground snow coverage for the winter without significantly warmer temperatures in the autumn are likely important for counteracting negative density-dependent effects on maternal fitness, reproductive success, and calf survival and body mass (Bonenfant et al. 2009).

Fall and winter conditions, such as the onset of winter in this study, not only affect reindeer herd and population recruitment, but also alter availability of vegetation early in the growing season, when damaged plants may be delayed in recovery and intrapopulation competition for resources is high among reindeer (Bårdsen and Tveraa 2012; Helle and Kojola 2008; Mårell et al. 2006). Dominant vegetation in sub-Arctic tundra will have difficulty recovering from recurrent sudden winter warming events when the availability of soil nitrogen is increased by summer warming (Aerts 2010). Refreezing of exposed vegetation during a winter with high snow-melting events contributed to the collapse of a reindeer population on Svalbard (Aanes et al. 2000, 2002). Enhanced vascular plant growth due to warmer temperatures during the growing season is likely to lead to reduced lichen cover, a major part of reindeer winter diet (Bjerke et al. 2011).

Herbivores in northern latitudes may therefore be required to adapt to changes in plant phenology in order to exploit high-quality forage efficiently (Zhao et al. 2019), particularly if winter warming events followed by severe freezes that seriously reduce food availability become more common.

Persistent changes and increased fluctuations in the Arctic ecosystem due to climate change are likely to complicate the relationship of reindeer mass to plant productivity and phenology, autumn and winter environmental conditions, maternal weight, and herd density over time. It is evident that relationships between environmental and density-dependent effects in the population dynamics of large Arctic herbivores are changing with global warming, but Arctic wild reindeer population dynamics may stabilize in the face of more frequent extreme winter events (Hansen et al. 2019a). Our results underscore that good conditions early in life through maternal effects along with robust, low density populations may be key for Arctic herbivores such as reindeer to withstand the density-dependent effects of extreme environmental variability brought about by climate change (Hansen et al. 2019a; Paoli et al. 2020). More importantly, our methods expand the usability of nonparametric regression models for effective summarization, modelling, and interpretation of spatiotemporal climate effects on animal populations, and our deployment of these methods for the analysis of a complex spatiotemporal plant-herbivore system illustrate their broad applicability for examining population-level responses to environmental variation and climate change at large spatial and temporal scales.

Supplementary Information The online version contains supplementary material available at https://doi.org/10.1007/s00442-022-05150-7.

Acknowledgements The authors are grateful to the comments and suggestions on early drafts of this work provided by Prof. F. Stephen Dobson.

Author contribution statement HEC, TT, and NY conceptualized the research. AS and TT gathered and organized the data. HEC designed and performed the analysis. HEC wrote the first version of the paper. TT, NY, and AS contributed to the final version.

Funding H.E.C. was supported by a U.S. National Science Foundation (NSF) predoctoral fellowship Grant No. NSF-DGE-1414475 and the Research Council of Norway (RCN) Grant No. 276395.

Availability of data and materials The datasets used and analysed for this study are available from the Harvard Dataverse at https://doi.org/10.7910/DVN/FTMDK6.

Code availability Code is available from a GitHub repository at https://github.com/hannahcorreia/reindeer-decomp. A permanent copy of the code used to produce the results for this study can be accessed at https://doi.org/10.5281/zenodo.6020919.

Declarations

Conflict of interest The authors declare no conflict of interests.

Ethics approval Not applicable.

Consent to participate Not applicable.

Consent for publication Not applicable.

References

Aanes R, Sæther B-E, Øritsland NA (2000) Fluctuations of an introduced population of Svalbard reindeer: the effects of density dependence and climatic variation. Ecography 23(4):437–443

Aanes R, Sæther B-E, Smith FM, Cooper EJ, Wookey PA, Øritsland NA (2002) The Arctic Oscillation predicts effects of climate change in two trophic levels in a high-arctic ecosystem. Ecol Lett 5(3):445–453

Aerts R (2010) Nitrogen-dependent recovery of subarctic tundra vegetation after simulation of extreme winter warming damage to Empetrum hermaphroditum. Glob Change Biol 16(3):1071–1081

Albon SD, Irvine RJ, Halvorsen O, Langvatn R, Loe LE, Ropstad E, Veiberg V, van der Wal R, Bjørkvoll EM, Duff EI, Hansen BB, Lee AM, Tveraa T, Stien A (2016) Contrasting effects of summer and winter warming on body mass explain population dynamics in a food-limited Arctic herbivore. Glob Change Biol 23(4):1374–1389

Augustin NH, Musio M, von Wilpert K, Kublin E, Wood SN, Schumacher M (2009) Modeling spatiotemporal forest health monitoring data. J Am Stat Assoc 104(487):899–911

Augustin NH, Trenkel VM, Wood SN, Lorance P (2013) Space-time modelling of blue ling for fisheries stock management. Environmetrics 24(2):109–119

Ballesteros M, Bårdsen B-J, Fauchald P, Langeland K, Stien A, Tveraa T (2013) Combined effects of long-term feeding, population density and vegetation green-up on reindeer demography. *Ecosphere* 4(4):art45

Bårdsen B-J (2017) Evolutionary responses to a changing climate: implications for reindeer population viability. Ecol Evol 7(15):5833–5844

Bårdsen B-J, Tveraa T (2012) Density-dependence vs. density-independence—linking reproductive allocation to population abundance and vegetation greenness. J Anim Ecol 81(2):364–376

Bjerke JW, Bokhorst S, Zielke M, Callaghan TV, Bowles FW, Phoenix GK (2011) Contrasting sensitivity to extreme winter warming events of dominant sub-arctic heathland bryophyte and lichen species. J Ecol 99(6):1481–1488

Bokhorst S, Bjerke JW, Bowles FW, Melillo J, Callaghan TV, Phoenix GK (2008) Impacts of extreme winter warming in the sub-arctic: growing season responses of dwarf shrub heathland. Glob Change Biol 14(11):2603–2612

Bonenfant C, Gaillard J, Coulson T, Festa-Bianchet M, Loison A, Garel M, Loe LE, Blanchard P, Pettorelli N, Owen-Smith N, Toit JD, Duncan P (2009) Chapter 5 empirical evidence of density-dependence in populations of large herbivores. Adv Ecol Res 41:313–357

Callaghan TV, Johansson M, Brown RD, Groisman PY, Labba N, Radionov V, Bradley RS, Blangy S, Bulygina ON, Christensen TR, Colman JE, Essery RLH, Forbes BC, Forchhammer MC, Golubev VN, Honrath RE, Juday GP, Meshcherskaya AV, Phoenix GK, Pomeroy J, Rautio A, Robinson DA, Schmidt NM, Serreze MC, Shevchenko VP, Shiklomanov AI, Shmakin AB, Sköld P, Sturm

M, Woo M-K, Wood EF (2011) Multiple effects of changes in arctic snow cover. Ambio 40(Suppl 1):32–45
Collado E, Bonet J, Camarero J, Egli S, Peter M, Salo K, Martínez-Peña F, Ohenoja E, Martín-Pinto P, Primicia I, Büntgen U, Kurttila M, de Rueda JO, de Aragón JM, Miina J, de Miguel S (2019) Mushroom productivity trends in relation to tree growth and climate across different european forest biomes. Sci Total Environ 689:602–615
Collins W, Smith T (1991). Effects of wind-hardened snow on foraging by reindeer (rangifer tarandus). *Arctic*, pp 217–222
Colman JE, Pedersen C, Hjermann DØ, Holand Ø, Moe SR, Reimers E (2003) Do wild reindeer exhibit grazing compensation during insect harassment? J Wildl Manage 67(1):11–19
Coull BA, Ruppert D, Wand MP (2001) Simple incorporation of interactions into additive models. Biometrics 57(2):539–545
Doiron M, Legagneux P, Gauthier G, Lévesque E (2013) Broad-scale satellite normalized difference vegetation index data predict plant biomass and peak date of nitrogen concentration in Arctic tundra vegetation. Appl Veget Sci 16(2):343–351
Dyrrdal AV, Saloranta T, Skaugen T, Stranden HB (2013) Changes in snow depth in Norway during the period 1961–2010. Hydrol Res 44(1):169–179
Finley AO (2011) Comparing spatially-varying coefficients models for analysis of ecological data with non-stationary and anisotropic residual dependence. Methods Ecol Evol 2(2):143–154
Gaillard J-M, Boutin J-M, Delorme D, Van Laere G, Duncan P, Lebreton J-D (1997) Early survival in roe deer: causes and consequences of cohort variation in two contrasted populations. Oecologia 112(4):502–513
Gaillard J-M, Festa-Bianchet M, Yoccoz NG (1998) Population dynamics of large herbivores: variable recruitment with constant adult survival. Trends Ecol Evol 13(2):58–63
Gordon IJ, Hester AJ, Festa-Bianchet M (2004) Review: the management of wild large herbivores to meet economic, conservation and environmental objectives. J Appl Ecol 41(6):1021–1031
GRASS Development Team (2017) Geographic Resources Analysis Support System (GRASS GIS) Software, Version 7.2. Open Source Geospatial Foundation
Hamel S, Garel M, Festa-Bianchet M, Gaillard J-M, Côté SD (2009) Spring normalized difference vegetation index (ndvi) predicts annual variation in timing of peak faecal crude protein in mountain ungulates. J Appl Ecol 46(3):582–589
Hansen BB, Aanes R, Herfindal I, Kohler J, Sæther B-E (2011) Climate, icing, and wild arctic reindeer: past relationships and future prospects. Ecology 92(10):1917–1923
Hansen BB, Gamelon M, Albon SD, Lee AM, Stien A, Irvine RJ, Sæther B-E, Loe LE, Ropstad E, Veiberg V, Grøtan V (2019a) More frequent extreme climate events stabilize reindeer population dynamics. Nat Commun 10(1):1616
Hansen BB, Pedersen ÅØ, Peeters B, Le Moullec M, Albon SD, Herfindal I, Sæther B-E, Grøtan V, Aanes R (2019b) Spatial heterogeneity in climate change effects decouples the long-term dynamics of wild reindeer populations in the high arctic. Glob Change Biol 25(11):3656–3668
Hastie TJ, Tibshirani RJ (1990) Generalized additive models. In: Monographs on statistics and applied probability, vol 43. Chapman and Hall, Ltd., London
Hastie T, Tibshirani R (1993) Varying-coefficient models. J R Stat Soc Ser B (Methodol) 55(4):757–796
Helle T, Kojola I (2008) Demographics in an alpine reindeer herd: effects of density and winter weather. Ecography 31(2):221–230
Hogda KA, Karlsen SR, Solheim I (2001) Climatic change impact on growing season in fennoscandia studied by a time series of noaa avhrr ndvi data. In: IGARSS 2001. Scanning the Present and Resolving the Future. Proceedings. IEEE 2001 International Geoscience and Remote Sensing Symposium (Cat. No. 01CH37217), vol 3, pp 1338–1340. IEEE
Hogrefe KR, Patil VP, Ruthrauff DR, Meixell BW, Budde ME, Hupp JW, Ward DH (2017) Normalized difference vegetation index as an estimator for abundance and quality of avian herbivore forage in Arctic Alaska. Remote Sens 9(12):1234
Holand Ø, Røed KH, Mysterud A, Kumpula J, Nieminen M, Smith ME (2003) The effect of sex ratio and male age structure on reindeer calving. J Wildl Manage 67(1):25–33
Høye TT, Post E, Meltofte H, Schmidt NM, Forchhammer MC (2007) Rapid advancement of spring in the high arctic. Curr Biol 17(12):R449–R451
Kauserud H, Stige LC, Vik JO, Økland RH, Høiland K, Stenseth NC (2008) Mushroom fruiting and climate change. Proc Natl Acad Sci 105(10):3811–3814
Kauserud H, Heegaard E, Semenov MA, Boddy L, Halvorsen R, Stige LC, Sparks TH, Gange AC, Stenseth NC (2010) Climate change and spring-fruiting fungi. Proc R Soc B: Biol Sci 277(1685):1169–1177
Kauserud H, Heegaard E, Halvorsen R, Boddy L, Høiland K, Stenseth NC (2011) Mushroom's spore size and time of fruiting are strongly related: is moisture important? Biol Lett 7(2):273–276
Keeling CD, Chin JFS, Whorf TP (1996) Increased activity of northern vegetation inferred from atmospheric CO_2 measurements. Nature 382(6587):146–149
Loe LE, Liston GE, Pigeon G, Barker K, Horvitz N, Stien A, Forchhammer M, Getz W, Irvine RJ, Lee A, Movik LK, Mysterud A, Pedersen ÅØ, Reinking AK, Ropstad E, Trondrud LM, Tveraa T, Veiberg V, Hansen BB, Albon S (2020) The neglected season: warmer autumns counteract harsher winters and promote population growth in arctic reindeer. Glob Change Biol 27:993–1002
Lussana C, Saloranta T, Skaugen T, Magnusson J, Tveito OE, Andersen J (2018) senorge2 daily precipitation, an observational gridded dataset over norway from 1957 to the present day. Earth Syst Sci Data 10(1):235–249
Mårell A, Hofgaard A, Danell K (2006) Nutrient dynamics of reindeer forage species along snowmelt gradients at different ecological scales. Basic Appl Ecol 7(1):13–30
Marin A, Sjaastad E, Benjaminsen TA, Sara MNM, Borgenvik EJL (2020) Productivity beyond density: a critique of management models for reindeer pastoralism in norway. Pastoralism 10(1):9
Masson-Delmotte V, Zhai P, Pörtner HO, Roberts D, Skea J, Shukla PR, Pirani A, Moufouma-Okia W, Péan C, Pidcock R, Connors S, Matthews JBR, Chen Y, Zhou X, Gomis MI, Lonnoy E, Maycock T, Tignor M, Waterfield T (eds) (2018) Global warming of 1.5° C.An IPCC Special Report on the impacts of global warming of 1.5°C above pre-industrial levels and related global greenhouse gas emission pathways, in the context of strengthening the global response to the threat of climate change, sustainable development, and efforts to eradicate poverty, chapter IPCC, 2018: Summary for Policymakers. World Meteorological Organization, Geneva, Switzerland, pp 32
MET Norway (2018) Norwegian Meteorological Institute: Cryo. Online. Data retrieved from Norwegian Meteorological Institute, http://www.senorge.no/
Moisen GG, Frescino TS (2002) Comparing five modelling techniques for predicting forest characteristics. Ecol Model 157(2):209–225
Movik LK (2018) Effects of spatio-temporal weather conditions in autumn and winter on body mass and behaviour of the high arctic svalbard reindeer (rangifer tarandus platyrhynchus). Master's thesis, Norwegian University of Life Sciences
Mu J, Wang G, Wang L (2018) Estimation and inference in spatially varying coefficient models. Environmetrics 29(1):e2485. e2485 env.2485

Ndegwa Mundia C, Murayama Y (2009) Analysis of land use/cover changes and animal population dynamics in a wildlife sanctuary in East Africa. Remote Sens 1(4):952–970

Oberbauer SF, Elmendorf SC, Troxler TG, Hollister RD, Rocha AV, Bret-Harte MS, Dawes MA, Fosaa AM, Henry GHR, Høye TT, Jarrad FC, Jónsdóttir IS, Klanderud K, Klein JA, Molau U, Rixen C, Schmidt NM, Shaver GR, Slider RT, Totland Ø, Wahren C-H, Welker JM (2013) Phenological response of tundra plants to background climate variation tested using the international tundra experiment. Philos Trans R Soc B: Biol Sci 368(1624):20120481

Oedekoven CS, Elston DA, Harrison PJ, Brewer MJ, Buckland ST, Johnston A, Foster S, Pearce-Higgins JW (2017) Attributing changes in the distribution of species abundance to weather variables using the example of British breeding birds. Methods Ecol Evol 8(12):1690–1702

Ogutu JO, Owen-Smith N, Piepho H-P, Dublin HT (2015) How rainfall variation influences reproductive patterns of african savanna ungulates in an equatorial region where photoperiod variation is absent. PLOS ONE 10(8):1

Owen-Smith N (1990) Demography of a large herbivore, the Greater Kudu Tragelaphus strepsiceros, in relation to rainfall. J Anim Ecol 59(3):893–913

Owen-Smith N, Mason DR, Ogutu JO (2005) Correlates of survival rates for 10 African ungulate populations: density, rainfall and predation. J Anim Ecol 74(4):774–788

Paoli A, Weladji RB, Holand Ø, Kumpula J (2018) Winter and spring climatic conditions influence timing and synchrony of calving in reindeer. PLOS ONE 13(4):1–21

Paoli A, Weladji RB, Holand O, Kumpula J (2019) The onset in spring and the end in autumn of the thermal and vegetative growing season affect calving time and reproductive success in reindeer. Curr Zool 66(2):123–134

Paoli A, Weladji RB, Holand O, Kumpula J (2020) Early-life conditions determine the between-individual heterogeneity in plasticity of calving date in reindeer. J Anim Ecol 89(2):370–383

Pape R, Löffler J (2015) Ecological dynamics in habitat selection of reindeer: an interplay of spatial scale, time, and individual animal's choice. Polar Biol 38(11):1891–1903

Park T, Ganguly S, Tømmervik H, Euskirchen ES, Høgda K-A, Karlsen SR, Brovkin V, Nemani RR, Myneni RB (2016) Changes in growing season duration and productivity of northern vegetation inferred from long-term remote sensing data. Environ Res Lett 11(8):084001

Pettorelli N, Vik JO, Mysterud A, Gaillard J-M, Tucker CJ, Stenseth NC (2005) Using the satellite-derived ndvi to assess ecological responses to environmental change. Trends Ecol Evol 20(9):503–510

Phillips AJ, Ciannelli L, Brodeur RD, Pearcy WG, Childers J (2014) Spatio-temporal associations of albacore CPUEs in the northeastern Pacific with regional SST and climate environmental variables. ICES J Mar Sci: Journal du Conseil 71(7):1717–1727

Pinzon J, Tucker C (2014) A non-stationary 1981–2012 avhrr ndvi3g time series. Remote Sens 6(8):6929–6960

Post E, Forchhammer MC (2008) Climate change reduces reproductive success of an Arctic herbivore through trophic mismatch. Philos Trans R Soc Lond B: Biol Sci 363(1501):2367–2373

Post E, Forchhammer MC, Bret-Harte MS, Callaghan TV, Christensen TR, Elberling B, Fox AD, Gilg O, Hik DS, Høye TT, Ims RA, Jeppesen E, Klein DR, Madsen J, McGuire AD, Rysgaard S, Schindler DE, Stirling I, Tamstorf MP, Tyler NJC, van der Wal R, Welker J, Wookey PA, Schmidt NM, Aastrup P (2009) Ecological dynamics across the arctic associated with recent climate change. Science 325(5946):1355–1358

R Core Team (2020) R: A Language and Environment for Statistical Computing. R Foundation for Statistical Computing, Vienna, Austria, v4.0.3 edition

Reimers E (2002) Calving time and foetus growth among wild reindeer in Norway. Rangifer 22(1):61

Roberts DR, Bahn V, Ciuti S, Boyce MS, Elith J, Guillera-Arroita G, Hauenstein S, Lahoz-Monfort JJ, Schröder B, Thuiller W, Warton DI, Wintle BA, Hartig F, Dormann CF (2017) Cross-validation strategies for data with temporal, spatial, hierarchical, or phylogenetic structure. Ecography 40(8):913–929

Sæther B-E (1997) Environmental stochasticity and population dynamics of large herbivores: a search for mechanisms. Trends Ecol Evol 12(4):143–149

Sala OE, Stuart Chapin III F, Armesto JJ, Berlow E, Bloomfield J, Dirzo R, Huber-Sanwald E, Huenneke LF, Jackson RB, Kinzig A, Leemans R, Lodge DM, Mooney HA, Oesterheld M, Poff NL, Sykes MT, Walker BH, Walker M, Wall DH (2000) Global biodiversity scenarios for the year 2100. Science 287(5459):1770–1774

Serneels S, Lambin EF (2001) Impact of land-use changes on the wildebeest migration in the northern part of the Serengeti-Mara ecosystem. J Biogeogr 28(3):391–407

Skogland T (1990) Density dependence in a fluctuating wild reindeer herd; maternal vs. offspring effects. Oecologia 84(4):442–450

Staton BA, Catalano MJ, Farmer TM, Abebe A, Dobson FS (2017) Development and evaluation of a migration timing forecast model for Kuskokwim River Chinook salmon. Fish Res 194(Supplement C):9–21

Stien A, Ims RA, Albon SD, Fuglei E, Irvine RJ, Ropstad E, Halvorsen O, Langvatn R, Loe LE, Veiberg V, Yoccoz NG (2012) Congruent responses to weather variability in high arctic herbivores. Biol Lett 8(6):1002–1005

Tablado Z, Fauchald P, Mabille G, Stien A, Tveraa T (2014) Environmental variation as a driver of predator-prey interactions. Ecosphere 5(12):art164

Tomaszewska MA, Nguyen LH, Henebry GM (2020) Land surface phenology in the highland pastures of montane central asia: Interactions with snow cover seasonality and terrain characteristics. Remote Sens Environ 240:111675

Torabi M (2014) Spatiotemporal modeling of odds of disease. Environmetrics 25(5):341–350

Tucker CJ, Pinzon JE, Brown ME, Slayback DA, Pak EW, Mahoney R, Vermote EF, Saleous NE (2005) An extended avhrr 8-km ndvi dataset compatible with modis and spot vegetation ndvi data. Int J Remote Sens 26(20):4485–4498

Turunen M, Soppela P, Kinnunen H, Sutinen ML, Martz F (2009) Does climate change influence the availability and quality of reindeer forage plants? Polar Biol 32(6):813–832

Tveraa T, Fauchald P, Henaug C, Yoccoz NG (2003) An examination of a compensatory relationship between food limitation and predation in semi-domestic reindeer. Oecologia 137(3):370–376

Tveraa T, Fauchald P, Gilles Yoccoz N, Anker Ims R, Aanes R, Arild Høgda K (2007) What regulate and limit reindeer populations in Norway? Oikos 116(4):706–715

Tveraa T, Stien A, Bårdsen B-J, Fauchald P (2013) Population densities, vegetation green-up, and plant productivity: impacts on reproductive success and juvenile body mass in reindeer. PLOS ONE 8(2):1–8

Tveraa T, Stien A, Brøseth H, Yoccoz NG (2014) The role of predation and food limitation on claims for compensation, reindeer demography and population dynamics. J Appl Ecol 51(5):1264–1272

Tyler NJC, Forchhammer MC, Øritsland NA (2008) Nonlinear effects of climate and density in the dynamics of a fluctuating population of reindeer. Ecology 89(6):1675–1686

van de Pol M, Bailey LD, McLean N, Rijsdijk L, Lawson CR, Brouwer L (2016) Identifying the best climatic predictors in ecology and evolution. Methods Ecol Evol 7(10):1246–1257

Veiberg V, Loe LE, Albon SD, Irvine RJ, Tveraa T, Ropstad E, Stien A (2017) Maternal winter body mass and not spring phenology determine annual calf production in an arctic herbivore. Oikos 126(7):980–987

Vistnes II, Nellemann C, Jordhøy P, Støen O-G (2008) Summer distribution of wild reindeer in relation to human activity and insect stress. Polar Biol 31(11):1307

Weladji RB, Steinheim G, Holand Ø, Moe SR, Almøy T, Ådnøy T (2003) Temporal patterns of juvenile body weight variability in sympatric reindeer and sheep. Annales Zoologici Fennici 40(1):17–26

Wood SN (2006) Generalized additive models. Texts in Statistical Science Series. Chapman & Hall/CRC, Boca Raton, FL. An introduction with R

Wood SN (2017) Generalized additive models: An Introduction with R. Texts in Statistical Science Series. 2 edn. Chapman & Hall/CRC, Boca Raton, FL

Wood SN, Pya N, Säfken B (2016) Smoothing parameter and model selection for general smooth models. J Am Stat Assoc 111(516):1548–1563

Woolford DG, Bellhouse DR, Braun WJ, Dean CB, Martell DL, Sun J (2011) A spatio-temporal model for people-caused forest fire occurrence in the Romeo Malette Forest. J Environ Stat 2(1):2–26

Zhao LZ, Colman AS, Irvine RJ, Karlsen SR, Olack G, Hobbie EA (2019) Isotope ecology detects fine-scale variation in svalbard reindeer diet: implications for monitoring herbivory in the changing arctic. Polar Biol 42(4):793–805